Hindawi Publishing Corporation
Journal of Spectroscopy
Volume 2015, Article ID 957868, 7 pages
http://dx.doi.org/10.1155/2015/957868

Research Article

Evaluation of Temper Embrittlement of 30Cr2MoV Rotor Steels Using Electrochemical Impedance Spectroscopy Technique

Zhang Shenghan, Lv Yaling, and Tan Yu

North China Electric Power University, Baoding 071000, China

Correspondence should be addressed to Zhang Shenghan; zhang_shenghan@yeah.net

Received 6 August 2014; Accepted 21 August 2014

Academic Editor: Tifeng Jiao

Copyright © 2015 Zhang Shenghan et al. This is an open access article distributed under the Creative Commons Attribution License, which permits unrestricted use, distribution, and reproduction in any medium, provided the original work is properly cited.

Temper embrittlement tends to occur in the turbine rotor after long running, which refers to the decrease in notch toughness of alloy steels in a certain temperature range (e.g., 400°C to 600°C). The severity of temper embrittlement must be monitored timely to avoid further damagement, and the fracture appearance transition temperature ($FATT_{50}$) is commonly used as an indicator parameter to characterize the temper embrittlement. Compared with conventional destructive methods (e.g., small punch test), nondestructive approaches have drawn significant attention in predicting the material degradation in turbine rotor steels without impairing the integrity of the components. In this paper, laboratory experiments were carried out based on a nondestructive method, electrochemical impedance spectroscopy (EIS), with groups of lab-charged specimens for predicting the temper embrittlement ($FATT_{50}$) of turbine rotor steel. The results show that there was a linear relationship of interfacial impedance of the specimens and their $FATT_{50}$ values. The predictive error based on the experiment study is within the range of ±15°C, indicating the predicting model is precise, effective, and reasonable.

1. Introduction

Thermal power stations are the most common electricity sources all over the world due to their low running costs and reliability. However, any failures in the main components (e.g., steam turbine rotor) of aged thermal power plants operating in many areas may cause significant costs, long downtime, and even the loss of life. The precisely predicting of the aging process or the remaining service life of turbine rotor is of great importance for safe operation and life extension [1].

Temper embrittlement in low alloy steels (e.g., Cr-Mo-V) of steamed turbine rotors is one of the typical material degradations (e.g., creep, fatigue, embrittlement, and corrosion) [2, 3] and is commonly characterized by fracture appearance transition temperature ($FATT_{50}$), at which the fracture surface of the material is 50% brittle or cleavage and 50% ductile [1]. The turbine rotor steel operated at a high temperature for long time may lose its flexibility and ductility as the segregation of metalloid impurities such as phosphorus (P), tin (Sn), and antimony (Sb), at the grain boundaries which reduces the cohesion at grain boundaries [4–6]. Among the impurity elements, phosphorus (P) is considered as the main impurity causing temper embrittlement [5, 7, 8]. If the increase of $FATT_{50}$ value is not detected in time, the rotor steel can be easily damaged or even broken and causes severe safety accidents [4]. Therefore, it is essential to make the accurate predictions and assessments on the temper embrittlement parameters of the turbine rotor material.

To date, different destructive and nondestructive methods have been developed to detect the $FATT_{50}$ value of turbine rotors, such as small punch test [1, 9–12], electromagnetic method [13], ultrasonic [14–16], auger electron spectroscopy [17, 18], electrochemical method [5, 19, 20], and chemical corrosion [19]. Destructive methods can provide accurate results of mechanical properties (e.g., yield stress, tensile strength, $FATT_{50}$, fracture toughness, and creep

properties) from the actual components [11, 12], but their application is highly-limited due to the damage to the turbine rotor.

As a relatively high-precision nondestructive detecting method, electrochemical approach has drawn significant attention in predicting the material degradation in turbine rotor steels without impairing the integrity of the components. Mao and Zhao investigated the electrochemical behaviors of type 321 austenitic stainless steel in sulfuric acid solution and found that the electrochemical polarization curves can be used to estimate the aging embrittlement degradation [21]. Komazaki et al. developed a methodology for thermal aging embrittlement and the results on electrochemical polarization measurements in 1N KOH solution revealed that the peak current density "I_p" value was found to be increasing linearly with the degree of embrittlement as evaluated by impact absorbed energy at 0°C [22, 23]. Anodic and single loop electrochemical potentiokinetic reactivation (SL-EPR) polarization curves of the embrittled specimens have been evaluated; difference in current density (IP2-E-Ipass-E) between active second peak and passive one in an anodic polarization curve of temper-embrittled specimens increases linearly with increase in FATT in the range of mode transfer over transgranular cleavage to intergranular of Charpy impact fracture [24]. Zhang et al. developed a genetic programming (GP) for $FATT_{50}$ prediction and single loop electrochemical polarization reactivation (EPR) test has been conducted [5]. The multiple correlation coefficient between predicted and measured $FATT_{50}$ was 0.990, indicating the model obtained by GP can be used in predicting temper embrittlement of new rotor materials with a precision of about ±20°C [5]. Bayesian neural network was proposed to model the temper embrittlement of steam turbine rotor in service, and the $FATT_{50}$ was predicted as a function of ratio of the two peak current densities (I_p/I_{pr}) tested by electrochemical potentiodynamic reaction method [25].

EIS, as an effective electrochemical method, originally was used to study the electrical response characteristic frequency of linear circuit network and has been used by more and more researchers to study the electrode process which could provide more information of interface structure than other methods [26–28].

In this paper, EIS method was employed to study the thermal embrittlement of turbine rotor and a multiple linear regression analysis on interfacial impedance and other relevant parameters was carried out to build a predict model of $FATT_{50}$. The predicted and measured values of $FATT_{50}$ were compared and the error was within an acceptable range, indicating an effective and reasonable model was obtained.

2. Experimental Method

2.1. Principle. The test specimens in this paper were lab-charged phosphorus-doped 30Cr2MoV rotor steel and the chemical composition was shown in Table 1.

To simulate the temper embrittlement during the long-term service of turbine rotor, step cooling treatment was used to promote the segregation of phosphorus to the grain boundary. Their $FATT_{50}$ values were measured by a stress test according to relevant national standard. The result would be used to verify the subsequent test. Impedance of the specimens was measured in a three-electrode system and analyzed by the equivalent circuit method. A predictive model was built based on the analysis results.

2.2. Experiment. $FATT_{50}$ values of specimens were measured by stress test and the result is shown in Table 2.

To measure the impedance of the specimens, a three-electrode system was employed. As shown in Figure 1, the specimen was cut into cube with side length of 12 mm and was welded on a piece of copper wire. The specimen cube acts as the working electrode in the experiment. In order for the reaction area of the working electrode to remain fixed, five sides of the cube, including some parts of the copper wire, were sealed with epoxy resin; the remaining side was covered with anticorrosion tape with a hole (diameter = 5 mm) after being grinded with sandpaper step by step to 2000#.

Platinum electrode was selected as auxiliary electrode and saturated calomel electrode was used as reference electrode. Electrolyte was made of 0.01 M Na_2MoO_4 with phosphoric deployed to the pH value of 5.5. The three-electrode system was placed in a water bath filled with circulating hot water of 25°C to maintain a constant temperature.

The three-electrode system was connected to the corresponding position of electrochemical workstation (model of PARTAT 2273). A computer equipped with software of that workstation was used to record measurements.

All specimens were anodic polarized; the result showed that those corrosion potentials are basically the same. In order to measure the EIS, AC potential with amplitude of 5 mV was applied to working electrode at the corrosion potential as input signal. Sixty frequencies were logarithmic sweeply selected from 100 kHz to 100 mHz. Impedance under that condition could be measured by comparing the measured output current with the input potential.

3. Results and Discussion

Figure 2 shows the Nyquist plot of measured impedance of specimen. The impedance was represented by a complex. The abscissa of plot in Figure 2 is the real part of the impedance, and the ordinate is the imaginary part. The results showed that the Nyquist plot of all specimens is similar. In the high frequency region, the plots were arcs in the first quadrant, but the centers of arcs were in the fourth quadrant. Some studies claimed that high frequency region was dynamics control district and the diameter of the arc represents the size of charge transfer resistance of the electrode reaction. The higher the diameter of arc, the more difficult the charge transfer in electrode reaction, and the slower the reaction. In the low frequency region, the plots were straight lines of different lengths. This region was considered mass transfer controlled district. If the line in this region was very long, the electrode reaction could be considered as led by mass transfer.

Table 1: Chemical composition of 30Cr2MoV rotor steel (wt%).

Sample	P	C	Si	Mn	S	Cr	Ni	Mo	Cu	V	As	Sn	Sb
41	0.045	0.28	0.36	0.66	0.013	1.62	0.06	0.62	0.08	0.29	0.013	0.004	0.0013
42	0.107	0.3	0.37	0.69	0.014	1.65	0.05	0.73	0.07	0.29	0.013	0.004	0.0015
43	0.063	0.28	0.36	0.69	0.014	1.68	0.05	0.68	0.1	0.29	0.015	0.006	0.0019
44	0.204	0.3	0.37	0.69	0.015	1.66	0.05	0.75	0.1	0.29	0.015	0.007	0.002
A2	0.065	0.28	0.43	0.68	0.012	1.79	0.28	0.7	0.08	0.3	0.013	0.004	0.0012
A3	0.019	0.24	0.4	0.62	0.001	1.6	0.25	0.69	0.12	0.27	0.007	0.008	0.0015

Table 2: The $FATT_{50}$ values of different rotor samples.

Sample	Original state	Heat-treated state	Difference
41	67.5	95.6	28.1
42	198.7	211.7	13
43	103.6	142.2	38.6
44	235	275.4	40.4
A2	82	127.1	45.1
A3	−70.9	−54.1	16.8

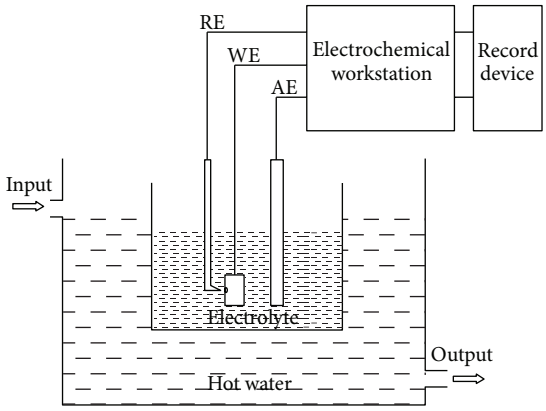

Figure 1: A three-electrode system for measuring the impedance of the specimens.

An equivalent circuit based on impedance plots was shown in Figure 3.

R_L is the solution impedance between working electrode and auxiliary electrode. CPE is constant-phase-element which could be expressed by parameters Y_0 and n. R_{ct} is the charge transfer impedance of the electrode reaction. W is mass transfer impedance and can be expressed by parameter Y_0'. The impedance of the equivalent circuit could be calculated by (1) as follows:

$$Z = Z_{R_L} + \frac{1}{Y_{\mathrm{CPE}} + Y_{(\mathrm{CPE}(R_{\mathrm{ct}}W))}} = R_L + \frac{1}{Y_0(j\omega)^{-n} + \left(1/\left(R_{\mathrm{ct}} + \left(1/Y_0'\sqrt{j\omega}\right)\right)\right)}. \quad (1)$$

The impedance value calculated by the formula matched well the experimental results. Figure 4 showed the calculated and measured curves, and the fitting error of each equivalent circuit component parameter was less than 5%.

By analyzing the component parameter values of equivalent circuit, it could be found that the solution impedance of specimens was essentially unchanged, but the interface impedance varied greatly. Figure 5 shows the linear relationship of interfacial impedance of specimen and its $FATT_{50}$ at a frequency of 100 kHz. The abscissa of Figure 5 was interfacial impedance value in ohms; ordinate was $FATT_{50}$ value in degree Celsius. Their fitting formula was in the upper left corner. The y in formula represented $FATT_{50}$ and x interfacial impedance. The R in formula is the correlation coefficient, and it was calculated as 0.836 by $R^2 = 0.6983$. $R_{\min}$, the correlation coefficient threshold, could be looked up from corresponding table as 0.567 [29]. Since R was greater than $R_{\min}$, it could be believed that there was a close linear relationship between the interfacial impedance and $FATT_{50}$, and the $FATT_{50}$ could be described by linear equations.

In addition to the interfacial impedance, $FATT_{50}$ also has linear correlationship with other parameters [29] which were shown in Table 3.

By multivariate linear regression analysis using excel software, the regression equation could be expressed by (2), where Z was interfacial impedance. One has

$$\mathrm{FATT}_{50} = -2002 + 1264 * Z + 178 * \mathrm{P} + 4106 * \mathrm{C} + 1318 * \mathrm{Mn} - 9214 * \mathrm{S} - 0.6 * \psi. \quad (2)$$

Significant test using Excel software showed that the equation was credible and there was significant linear relationship between $FATT_{50}$ and other variables.

Table 3 shows that the residuals of predicted value were ±15°C, the error was small, and the model was reasonable and effective.

4. Conclusions

In this work, the EIS of turbine rotor at the corrosion potential in 0.01 M Na_2MoO_4 was studied through laboratory experiments, and the following conclusions are obtained. The electrode reaction of rotor in electrolyte could be represented by an equivalent circuit. The total impedance of the circuit

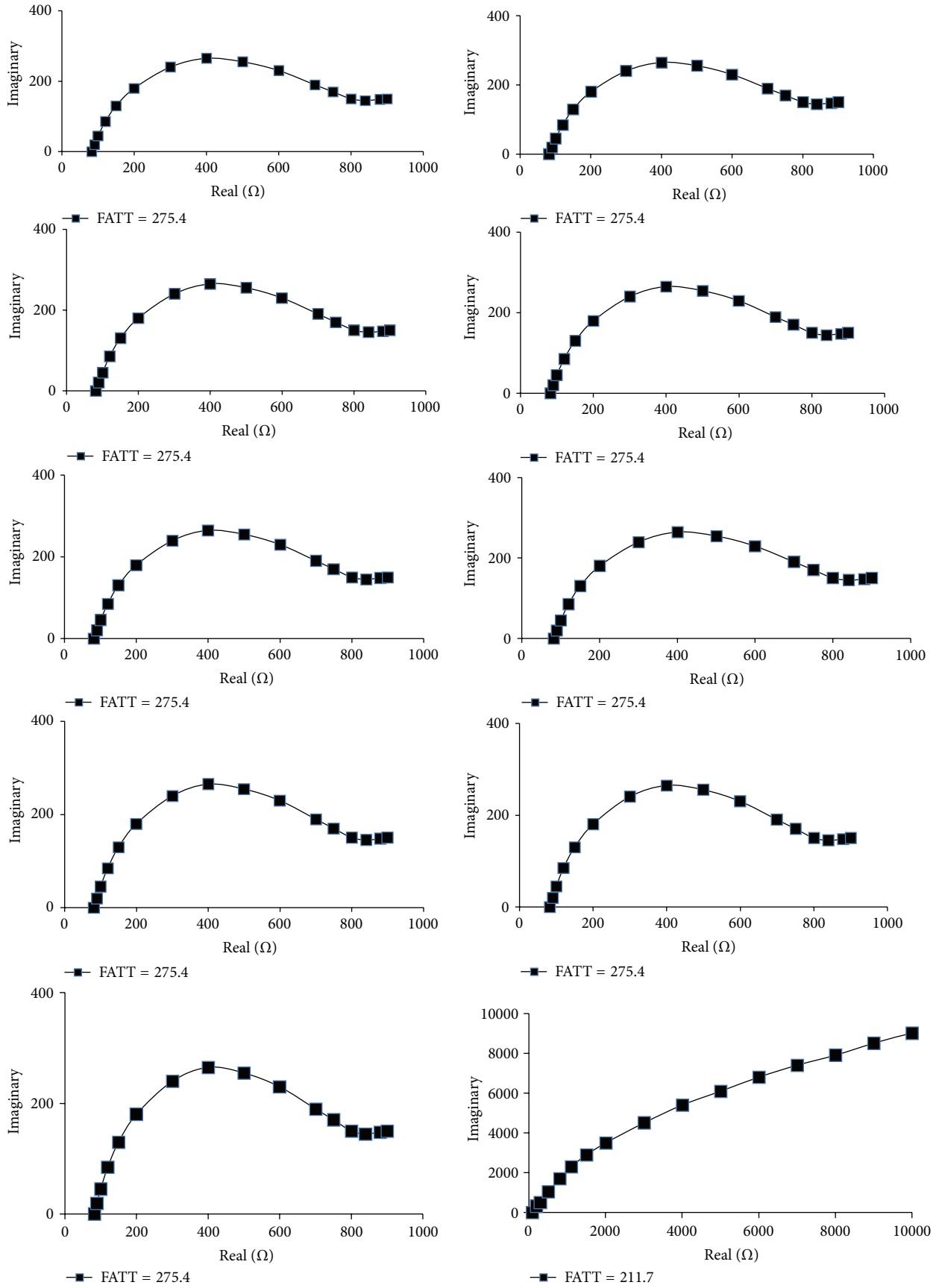

(a)

Figure 2: Continued.

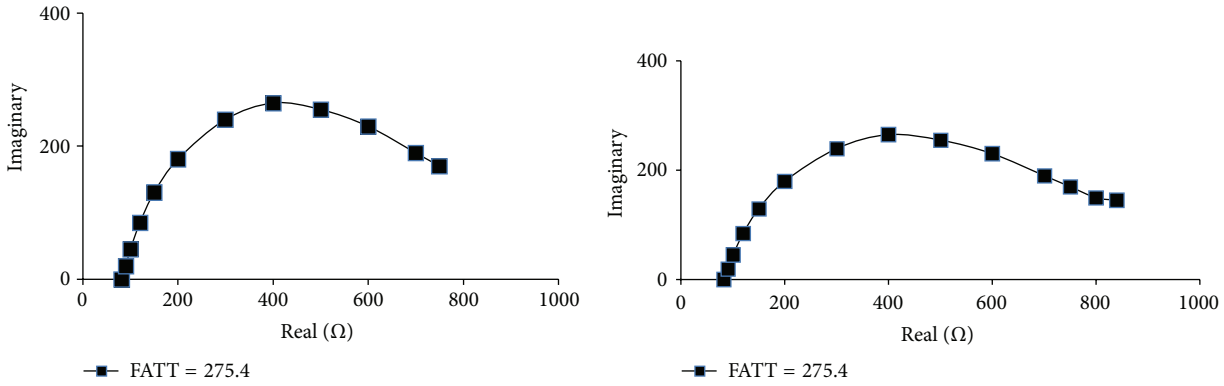

(b)

Figure 2: Nyquist diagrams of the impedance of different samples.

Table 3: $FATT_{50}$-related parameters.

Sample	Measured $FATT_{50}$	Impedance Z (Ω)	P (%)	C (%)	Mn (%)	S (%)	Reduction ψ (%)	Predicted value	Difference
A31	−70.9	0.07	0.019	0.24	0.62	0.001	72.2	−73.432	−2.532
A32	−54.1	0.09	0.019	0.24	0.62	0.001	71.33	−48.674	5.426
411	67.5	0.1	0.045	0.28	0.66	0.013	64.47	70.87	3.37
A21	82	0.09	0.065	0.28	0.68	0.012	60.3	94.862	12.862
412	95.6	0.12	0.045	0.28	0.66	0.013	62.33	94.866	−0.734
431	103.6	0.11	0.063	0.28	0.69	0.014	56.57	112.3	8.7
A22	127.1	0.11	0.065	0.28	0.68	0.012	52.57	115.504	−11.596
432	142.2	0.13	0.063	0.28	0.69	0.014	55.33	136.836	−5.364
421	198.7	0.11	0.107	0.3	0.69	0.014	52.8	199.99	1.29
422	211.7	0.12	0.107	0.3	0.69	0.014	54.17	213.452	1.752
441	235	0.13	0.204	0.3	0.69	0.015	46.65	229.632	−5.368
442	275.4	0.18	0.204	0.3	0.69	0.015	30.5	283.142	7.742

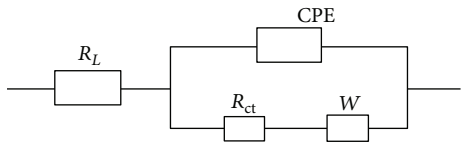

Figure 3: Constructed equivalent circuit in accordance with Figure 1.

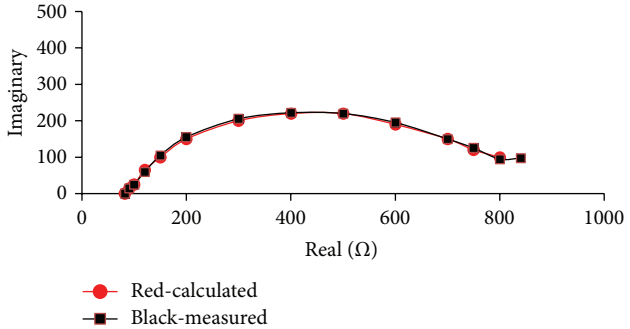

Figure 4: Comparison of the calculated and measured curve.

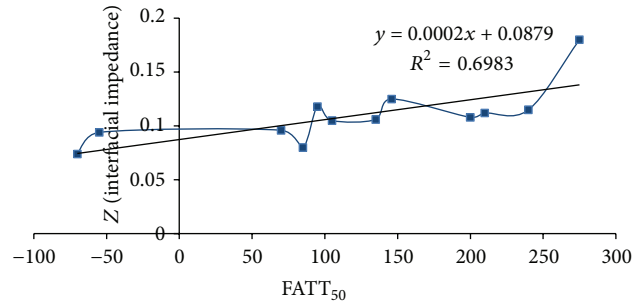

Figure 5: Relationship of interface impedance and $FATT_{50}$ values.

includes two parts: solution impedance between working electrode and auxiliary electrode and interfacial impedance between the rotor and electrolyte. At higher frequency, there is a linear relationship between the interfacial impedance and its $FATT_{50}$. The larger the interfacial impedance value, the lower the $FATT_{50}$. An effective predictive model could be built by a series of parameters, and the error is small enough indicating the model is reasonable and effective.

Conflict of Interests

The authors declare that there is no conflict of interests regarding the publication of this paper.

Acknowledgment

This paper is supported by the "Fundamental Research Funds for the Central Universities of China" (Grant no. 13MS85).

References

[1] J. S. Ha and E. Fleury, "Small punch tests to estimate the mechanical properties of steels for steam power plant: II. Fracture toughness," *International Journal of Pressure Vessels and Piping*, vol. 75, no. 9, pp. 707–713, 1998.

[2] Y. Kadoya, T. Goto, M. Takei, N. Haruki, T. Ikuno, and Y. Nishimura, "Nondestructive evaluation of temper embrittlement in Cr-Mo-V rotor steel," *Transactions of the Japan Society of Mechanical Engineers Part A*, vol. 57, no. 537, pp. 1085–1090, 1991.

[3] H. Uemura and M. Kohno, "Temper embrittlement characteristic of Cr-Mo-V steel steam turbine rotors in long term service," *Journal of the Iron and Steel Institute of Japan*, vol. 93, no. 4, pp. 324–329, 2007.

[4] Y.-M. Chen, Y. Long, Z.-G. Han, and Y.-H. Wang, "Predict the temper embrittlement extent of turbine rotor steel by using chemical corrosion method," in *Proceedings of the Asia-Pacific Power and Energy Engineering Conference (APPEEC '09)*, Wuhan, China, March 2009.

[5] S.-H. Zhang, Y.-Z. Fan, Y.-M. Chen, and S.-L. Zhou, "A new nondestructive test technique for predicting the temper embrittlement of turbine rotor steel with genetic programming," in *Proceedings of the IEEE International Conference on Industrial Technology (ICIT '05)*, pp. 768–771, Hong Kong, December 2005.

[6] A. Fujita, M. Shinohara, H. Yokota, K. Kaku, K. Soeda, and Y. Kuroda, "Effect of chemical composition and manufacturing procedure on toughness of CrMoV HP rotor forgings," *Journal of the Iron and Steel Institute of Japan*, vol. 84, no. 3, pp. 236–241, 1998.

[7] J. Kameda and R. Ranjan, "Nondestructive evaluation of steels using acoustic and magnetic barkhausen signals-I. Effect of carbide precipitation and hardness," *Acta Metallurgica*, vol. 35, no. 7, pp. 1515–1526, 1987.

[8] J. Kameda and R. Ranjan, "Nondestructive evaluation of steels using acoustic and magnetic barkhausen signals-II. Effect of intergranular impurity segregation," *Acta Metallurgica*, vol. 35, no. 7, pp. 1527–1531, 1987.

[9] A. Shekhter, S. Kim, D. G. Carr, A. B. L. Croker, and S. P. Ringer, "Assessment of temper embrittlement in an ex-service 1Cr-1Mo-0.25V power generating rotor by Charpy V-Notch testing, KIc fracture toughness and small punch test," *International Journal of Pressure Vessels and Piping*, vol. 79, no. 8–10, pp. 611–615, 2002.

[10] S.-I. Komazaki, T. Shoji, and K. Takamura, "Evaluation of thermal aging embrittlement in directionally solidified Ni-base superalloy by small punch test," *Journal of Engineering Materials and Technology, Transactions of the ASME*, vol. 127, no. 4, pp. 476–482, 2005.

[11] K. Turba, R. C. Hurst, and P. Hähner, "Anisotropic mechanical properties of the MA956 ODS steel characterized by the small punch testing technique," *Journal of Nuclear Materials*, vol. 428, no. 1–3, pp. 76–81, 2012.

[12] X. Mao, T. Shoji, and H. Takahashi, "Characterization of fracture behavior in small punch test by combined recrystallization-etch method and rigid plastic analysis," *Journal of Testing and Evaluation*, vol. 15, no. 1, pp. 30–37, 1987.

[13] G. Dobmann, "NDE for material characterisation of ageing due to thermal embrittlement, fatigue and neutron degradation," *International Journal of Materials and Product Technology*, vol. 26, no. 1-2, pp. 122–139, 2006.

[14] H. Jeong, S.-H. Nahm, K.-Y. Jhang, and Y.-H. Nam, "Evaluation of fracture toughness degradation of CrMoV rotor steels based on ultrasonic nonlinearity measurements," *KSME International Journal*, vol. 16, no. 2, pp. 147–154, 2002.

[15] H. Jeong, S.-H. Nahm, K.-Y. Jhang, and Y.-H. Nam, "A nondestructive method for estimation of the fracture toughness of CrMoV rotor steels based on ultrasonic nonlinearity," *Ultrasonics*, vol. 41, no. 7, pp. 543–549, 2003.

[16] C.-H. Hsu, H.-Y. Teng, and S.-C. Chiu, "Ultrasonic evaluation of temper-embrittlement for martensitic stainless steel," *Materials Transactions*, vol. 44, no. 11, pp. 2363–2368, 2003.

[17] R. Ding, A. Islam, S. Wu, and J. Knott, "Effect of phosphorus segregation on fracture properties of two quenched and tempered structural steels," *Materials Science and Technology*, vol. 21, no. 4, pp. 467–475, 2005.

[18] S. H. Song, J. Wu, L. Q. Weng, and T. H. Xi, "Phosphorus grain boundary segregation under an intermediate applied tensile stress in a Cr-Mo low alloy steel," *Materials Science and Engineering A*, vol. 520, no. 1-2, pp. 97–100, 2009.

[19] Y. Z. Fan, Y. M. Chen, and S. H. Zhang, "Development of nondestructive inspecting of temper embrittlement of turbine roter steel," *Turbine Technology*, Article ID 100125884, 2004.

[20] Y. Kadoya, T. Goto, M. Takei, N. Haruki, K. Ikuno, and Y. Nishimura, "Nondestructive evaluation of temper embrittlement in Cr-Mo-V rotor steel," *The American Society of Mechanical Engineers, Power Division (Publication) PWR*, vol. 13, pp. 229–234, 1991.

[21] X. Mao and W. Zhao, "Electrochemical polarization method to detect aging embrittlement of 321 stainless steel," *Corrosion*, vol. 49, no. 4, pp. 335–342, 1993.

[22] S.-I. Komazaki, S. Kishi, T. Shoji, H. Chiba, and K. Suzuki, "Thermal aging embrittlement of tungsten-alloyed 9%Cr ferritic steels and electrochemical evaluation," *Materials Science Research International*, vol. 9, no. 1, pp. 42–49, 2003.

[23] S.-I. Komazaki, S. Kishi, T. Shoji, H. Chiba, and K. Suzuki, "Thermal aging embrittlement of W alloyed 9%Cr ferritic steels and its evaluation by electrochemical technique," *Journal of the Society of Materials Science*, vol. 49, no. 8, pp. 919–926, 2000.

[24] T. Shibuya and T. Misawa, "Electrochemical evaluation of the degree of temper-embrittlement with mode transfer in impact fracture surface of 2.25Cr-1Mo low alloy steels," *Corrosion Engineering*, vol. 48, no. 3, pp. 146–154, 1999.

[25] S.-H. Zhang, Y.-Z. Fan, and Y.-M. Chen, "Predicting the temper embrittlement of steam turbine rotor steels with Bayesian neural network," in *Proceedings of the IEEE International Conference on Industrial Technology (ICIT '05)*, pp. 991–994, Hong Kong, December 2005.

[26] K. Darowicki, S. Krakowiak, and P. Ślepski, "Evaluation of pitting corrosion by means of dynamic electrochemical impedance spectroscopy," *Electrochimica Acta*, vol. 49, no. 17-18, pp. 2909–2918, 2004.

[27] C. Boissy, C. Alemany-Dumont, and B. Normand, "EIS evaluation of steady-state characteristic of 316L stainless steel passive film grown in acidic solution," *Electrochemistry Communications*, vol. 26, no. 1, pp. 10–12, 2013.

[28] S. Krakowiak, K. Darowicki, and P. Slepski, "Impedance investigation of passive 304 stainless steel in the pit pre-initiation state," *Electrochimica Acta*, vol. 50, no. 13, pp. 2699–2704, 2005.

[29] J. T. Zhang, *Nondestructive Method for the Evaluation of the Embrittlement of the Turbine Rotor Steels*, North China Electric Power University, Baoding, China, 2004.

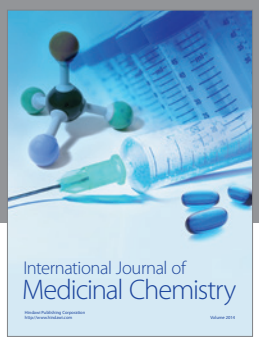

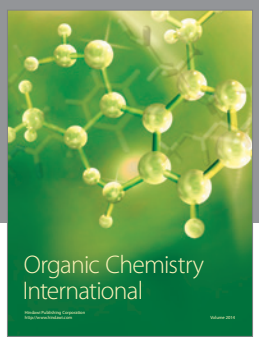

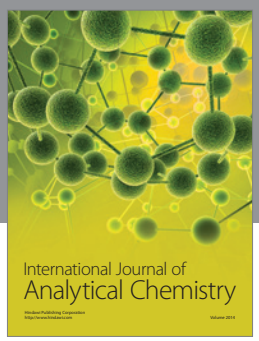

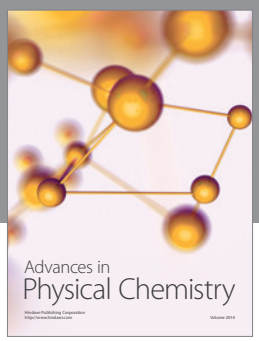

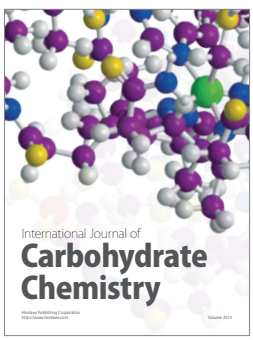

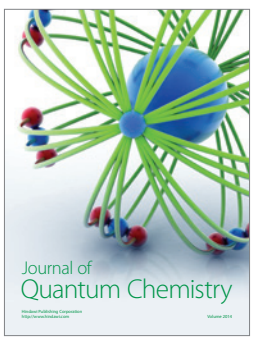

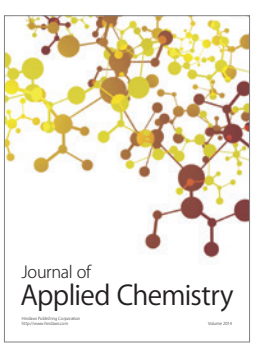

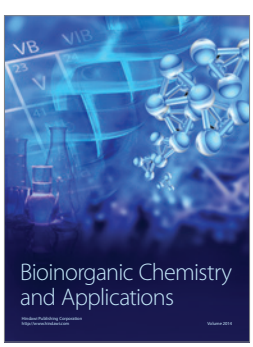

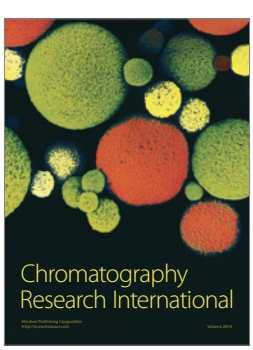

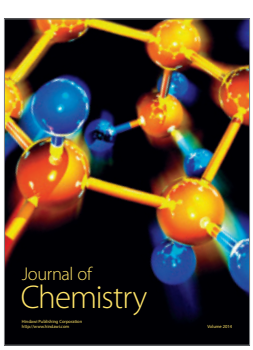

Hindawi

Submit your manuscripts at
http://www.hindawi.com